

Piezoelectricity and ballistic heat flow

G. L. Koos and J. P. Wolfe

*Physics Department and Materials Research Laboratory, University of Illinois
at Urbana-Champaign, Urbana, Illinois 61801*

(Received 12 December 1983)

We have examined the influence of piezoelectricity on the propagation of ballistic heat pulses in a lithium niobate crystal cooled to low temperatures. The phonon-imaging method reveals a ballistic flux pattern which cannot be explained simply in terms of the constant-field elastic tensor. The effect of introducing piezoelectrically stiffened elastic constants into the phonon-focusing calculation is striking. For example, caustics are introduced into the flux pattern for fast transverse phonons, in good agreement with the observations.

Piezoelectricity is the property of certain crystals such as quartz to couple electrical and mechanical fields.¹ Such crystals lack a center of inversion symmetry. A mechanical force applied to a piezoelectric crystal produces an electric polarization proportional to the strain, and conversely an applied electric field produces a strain in the crystal. In this paper we demonstrate that piezoelectricity can greatly affect the propagation of heat in a crystal. Our study of thermal phonons is a natural extension of continuum elasticity theory with piezoelectricity included. However, to our knowledge, there have been no previous attempts to show the influence of piezoelectricity on thermal energy flow. We find that in a highly piezoelectric crystal such as lithium niobate (LiNbO₃) the electromechanical coupling constants enter strongly into the anisotropic propagation of ballistic heat pulses at low temperatures.

This study was made possible by the recent development of phonon-imaging methods, which provide a two-dimensional representation of the ballistic heat flux emanating from a point source.² Even for crystals with nearly isotropic elasticity, highly anisotropic flux patterns are predicted—an effect known as phonon focusing. Thus crystals such as germanium, sapphire, and lithium fluoride have been shown to exhibit strongly anisotropic heat patterns which are predictable from the known elastic constants. Previous phonon-focusing calculations³ of the piezoelectric crystal quartz (SiO₂) did not consider the effect of piezoelectricity on thermal flux in this crystal. The predicted phonon-flux anisotropies were in fairly good agreement with a phonon-imaging experiment.⁴ For the present study, however, we have chosen a crystal which is considerably more piezoelectric than quartz, and we find that a proper inclusion of piezoelectric coupling is essential for an understanding of the ballistic heat-flow pattern.

Phonons in a typical heat pulse with temperature ~ 10 K have wavelengths greater than 100 Å; thus the continuum elasticity theory is applicable. For a nonpiezoelectric material a description of elastic waves begins with the generalized Hooke's law:

$$\sigma_{ij} = C_{ijmn} S_{mn} \quad (1)$$

where σ_{ij} is the stress applied in the i th direction to the j th plane, C_{ijmn} are the elastic stiffness constants, $S_{mn} \equiv \frac{1}{2}(\partial u_n / \partial x_m + \partial u_m / \partial x_n)$ is the strain tensor, and \bar{u} is the displacement of the medium from equilibrium at position \bar{x} . For a crystal of density ρ , the equation of motion

$\rho(\partial^2 u_i / \partial t^2) = \partial \sigma_{ij} / \partial x_j$ has a plane-wave solution, $\bar{u} = \bar{u}_0 \exp[i(\omega t - \bar{k} \cdot \bar{x})]$, which yields the Christoffel equation⁵

$$(C_{ijmn} k_j k_m - \rho \omega^2 \delta_{in}) u_n = 0 \quad (2)$$

The solution of this equation for a given phonon frequency ω results in three sheets of allowed wave vectors corresponding to the longitudinal (L), slow transverse (ST), and fast transverse (FT) phonon modes.

Figure 1 shows the ST and FT constant-frequency (or slowness) surfaces for lithium niobate, assuming the known elastic constants under constant electric field.⁶ Lithium niobate has trigonal symmetry, implying that there are six independent elastic constants. In Fig. 1, the z axis is the threefold crystal axis and the yz plane is a reflection plane. The slow transverse surface is composed of large totally convex regions bordered by saddle regions and six very small totally concave regions of different curvature, and thus correspond to a total Gaussian curvature of zero. Normals to the surface along these zero-curvature lines define group velocity directions of mathematically infinite phonon flux. Stated simply, the ratio of the k -space solid angle to the corresponding V -space solid angle at a zero-curvature point on the slowness surface is infinite. The FT surface is seen to be totally convex, thus no caustics would be expected in the FT phonon flux.

The phonon flux predicted by these constant-frequency surfaces can be obtained by selecting a large number of randomly oriented k vectors, determining the corresponding group vectors, and projecting these vectors from one point in the crystal to a selected crystal surface. Such a Monte Carlo image is shown in Fig. 1(c), which corresponds to a surface with normal 37° from the z axis in the yz plane. Both FT and ST modes are included in the calculation. The sharp features in this figure are caustics in ST phonon flux.

Of course, this calculation is not valid for a piezoelectric crystal, in which a phonon consists of both propagating mechanical and electric fields. Hooke's law must be modified to include the effect of the nonconstant local electric field E_r . That is,

$$\sigma_{ij} = C_{ijmn} S_{mn} - e_{ijr} E_r \quad (3)$$

where e_{ijr} are the piezoelectric stress constants. With the assumption of no free charges and neglecting magnetic induction, a modified Christoffel equation can be generated,¹

with C_{ijmn} replaced by a "stiffened" set of elastic constants,

$$C_{ijmn}^{\text{eff}} = C_{ijmn} + \frac{k_r e_{ijr} k_l e_{lmn}}{\epsilon_{lr} k_r k_l}, \quad (4)$$

where k_i are Cartesian components of the phonon wave vector and ϵ_{lr} is the dielectric tensor under constant strain. Thus the effect of piezoelectricity is to introduce elastic "constants" which depend upon the wave-vector direction.

By substituting these wave-vector-dependent elastic constants for C_{ijmn} into Eq. (2), we can again solve for the constant-frequency surfaces and parabolic lines of a given

piezoelectric material. Of course, the calculation is much more complex because it involves computing the first and second derivatives of the $C_{ijmn}^{\text{eff}} k_j k_m$ with respect to the wave-vector components. As in the nonpiezoelectric case, such derivatives are required for determining the group velocity vector and the Gaussian curvature.² We have carried out these calculations for the case of lithium niobate, using previously measured values of the piezoelectric constants,⁶ and the resulting slowness surfaces and predicted phonon-flux pattern are shown in Fig. 2. Comparison with Fig. 1 shows that the effect of the piezoelectric coupling is quite pronounced. The most striking change is that the FT sheet now has parabolic lines. A large saddle region has developed about the xy plane and this mode now displays singularities in flux.

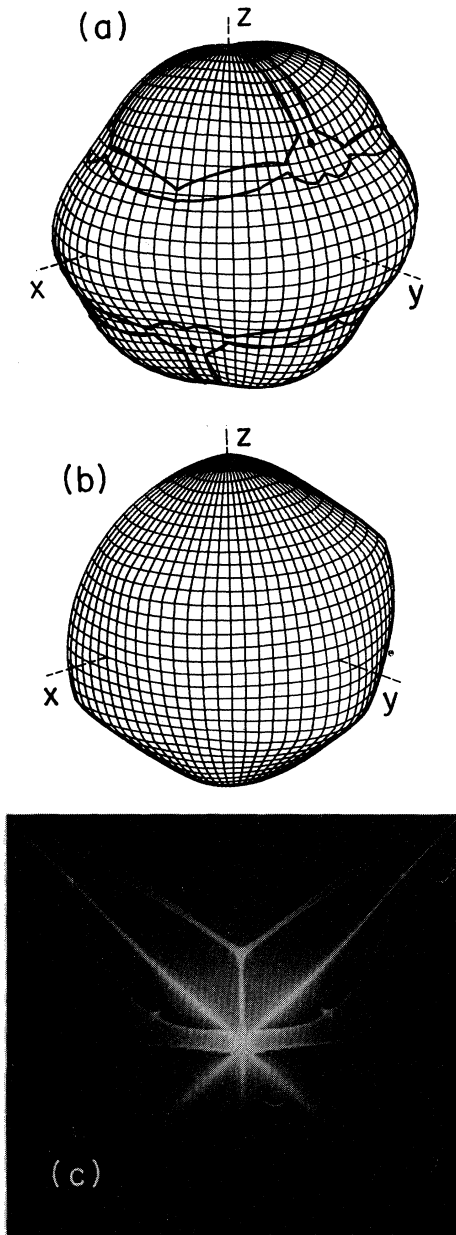


FIG. 1. Slowness surfaces obtained by using the constant-field elastic tensor of LiNbO_3 , i.e., neglecting piezoelectricity. Heavy lines indicate zero Gaussian curvature and they separate convex, saddle, and concave regions. (a) ST model. (b) FT mode. (c) Predicted phonon-flux pattern extending $\pm 71^\circ$ in propagation angle both horizontally and vertically.

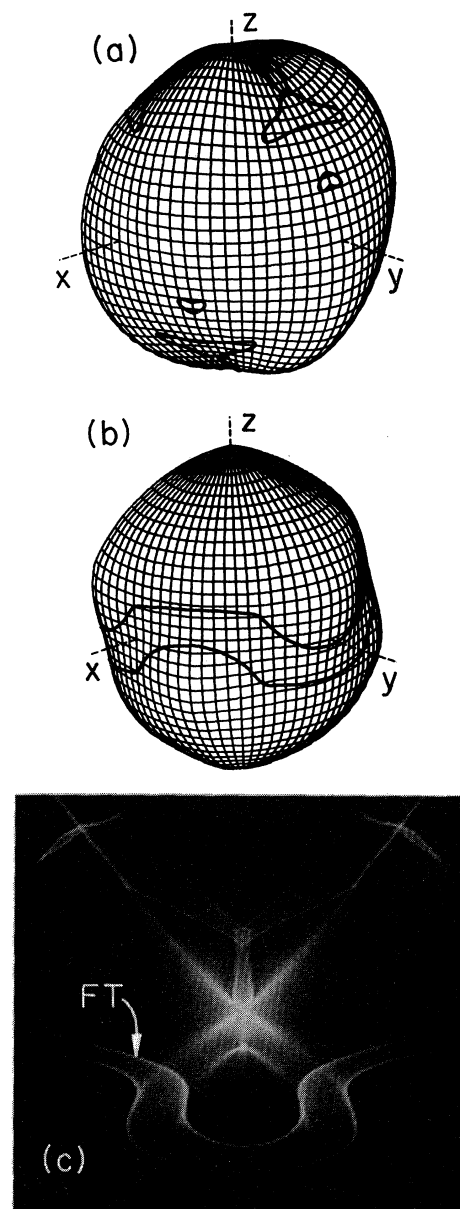


FIG. 2. Slowness surfaces obtained for LiNbO_3 , including the piezoelectric effect. (a) ST mode. (b) FT mode. (c) Predicted phonon-flux pattern extending $\pm 71^\circ$ horizontally and vertically.

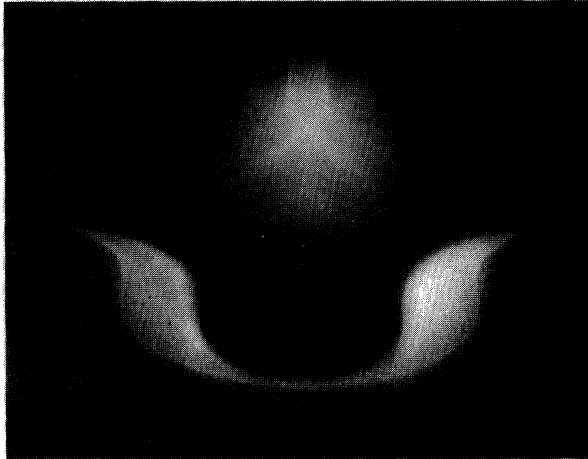


FIG. 3. Ballistic phonon image obtained with a broad time gate to include both ST and FT modes over a 50° range of propagation angles.

To compare these predictions with experiment we have chosen a lithium niobate crystal⁷ of 3-mm thickness having polished surfaces normal to $(\theta, \phi) = (37^\circ, 90^\circ)$, where the angles are defined with respect to the z and x axes. One of the polished faces has a 2000-Å copper film deposited on it, and the other face has a small ($50 \times 50 \mu\text{m}^2$) aluminum bolometer evaporated at its center. The phonon-imaging experiment is performed in the usual way by scanning a pulsed laser beam across the metallized surface of the crystal, which is immersed in superfluid helium at the superconducting transition of the bolometer. The intensity of the ballistic heat pulses detected by the bolometer is recorded in a 256×256 array and stored in a computer. The recorded image is played out on a television monitor and a photograph of the monitor is shown in Fig. 3. The image agrees quite well with one of the phonon-focusing calculations above, namely, the one with piezoelectricity properly included. The curved belt associated with FT phonons is clearly visible in the lower half of the image. The upper cusped structure is associated with the slow transverse phonons.

It is interesting to examine how the topological changes associated with piezoelectricity come about. We can hypothetically decrease the piezoelectricity in a gradual way by simply multiplying all of the piezoelectric constants by a scale factor f , which is varied between 1 and 0. This corresponds to a continuous change from Eq. (3) to Eq. (1). Figure 4 shows a cross section in the yz plane of the transverse slowness surface for various f . The inner (FT) and outer (ST) sheets meet at conic points, labeled C_i .

As f is increased from zero, the conic point C_1 which begins at $\theta_k = 115.4^\circ$ moves to 66° for $f = 1$. The motions of this conic point coincide with the breakup of the ST saddle region into several islands, as seen in Figs. 1(a) and 2(a). At $f = 0.95$, the ST and FT sheets of this surface touch

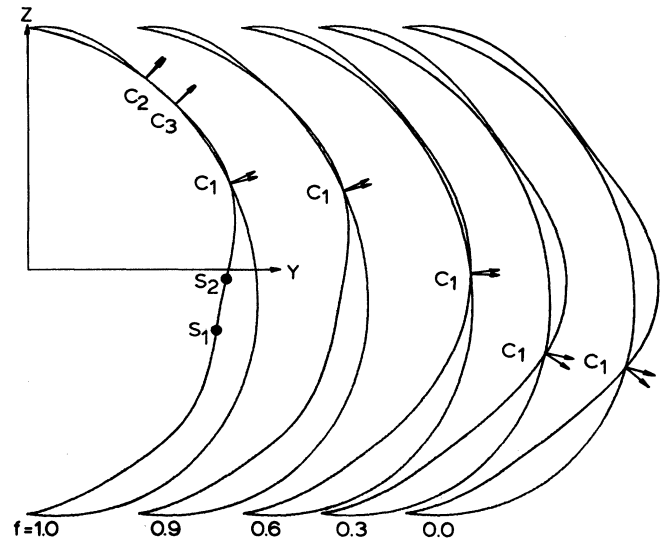


FIG. 4. Cross sections in the yz plane of the FT (inner) and ST (outer) sheets of the slowness surface. The changes in the shape of these surfaces as the piezoelectric coupling constants in Eq. (4) are gradually (hypothetically) increased from zero can be characterized by conic points C_i , where the two sheets touch, and singular points S_i , where the curvature vanishes (see also Fig. 2.)

each other at $\theta_k \approx 37^\circ$ and produce two new conic points C_2 and C_3 which move to $\theta_k = 3.1^\circ$ and 40.9° for $f = 1.0$. The FT sheet, which would have no saddle regions for $f = 0$, develops a saddle region, bordered by parabolic (singular flux) points S_1 and S_2 , for $f > 0.9$. This study shows that the motion of conic and singular points is a useful way to describe the topological changes in an acoustic surface as some control parameter is adjusted. We see that conic points are created or annihilated in pairs.

In conclusion, we have found that the piezoelectric effect can have a pronounced influence on the ballistic heat flow through dielectric crystals at low temperatures. For lithium niobate the effect is large, creating singularities in the fast transverse mode when the appropriate stiffened elastic constants are used. We have conducted a similar study for α quartz, and find that the smaller electromechanical coupling associated with this crystal has a small but detectable effect on the ballistic phonon pattern. Our study also suggests the potential of phonon imaging for characterizing the electromechanical properties of electrically active crystals.

We thank A. G. Every for suggesting lithium niobate and S. E. Hebboul for performing a preliminary experiment. G. A. Northrop provided valuable advice on both experimental and theoretical aspects of this work. This research was supported by the National Science Foundation under the Materials Research Laboratory Grant No. DMR-80-20250.

¹W. G. Cady, *Piezoelectricity* (McGraw-Hill, New York, 1946); B. A. Auld, *Acoustic Fields and Waves in Solids* (Wiley, New York, 1973).

²G. A. Northrop and J. P. Wolfe, *Phys. Rev. B* **22**, 6196 (1980).

³F. Rosch and O. Weis, *Z. Phys. B* **25**, 101 (1976).

⁴R. Eichele, R. P. Heubener, and H. Seifert, *Z. Phys. B* **48**, 89

(1982).

⁵A. G. Every, *Phys. Rev. B* **24**, 3456 (1981).

⁶R. T. Smith and F. S. Welsh, *J. Appl. Phys.* **42**, 2219 (1971).

⁷rf-transducer crystal grown by Crystal Technology, Palo Alto, CA and donated by W. Baronian of Intra Action Corporation.

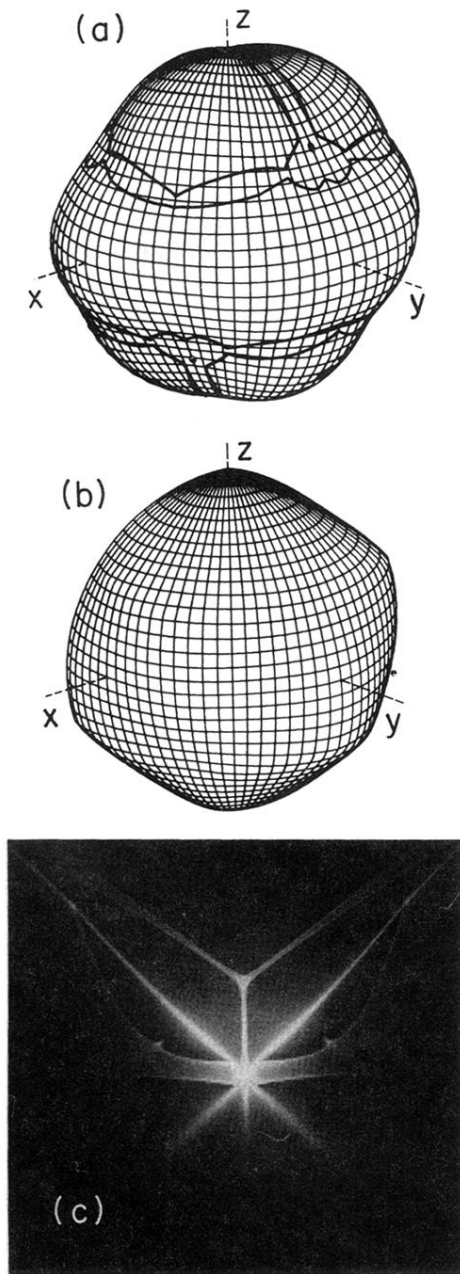


FIG. 1. Slowness surfaces obtained by using the constant-field elastic tensor of LiNbO_3 , i.e., neglecting piezoelectricity. Heavy lines indicate zero Gaussian curvature and they separate convex, saddle, and concave regions. (a) ST model. (b) FT mode. (c) Predicted phonon-flux pattern extending $\pm 71^\circ$ in propagation angle both horizontally and vertically.

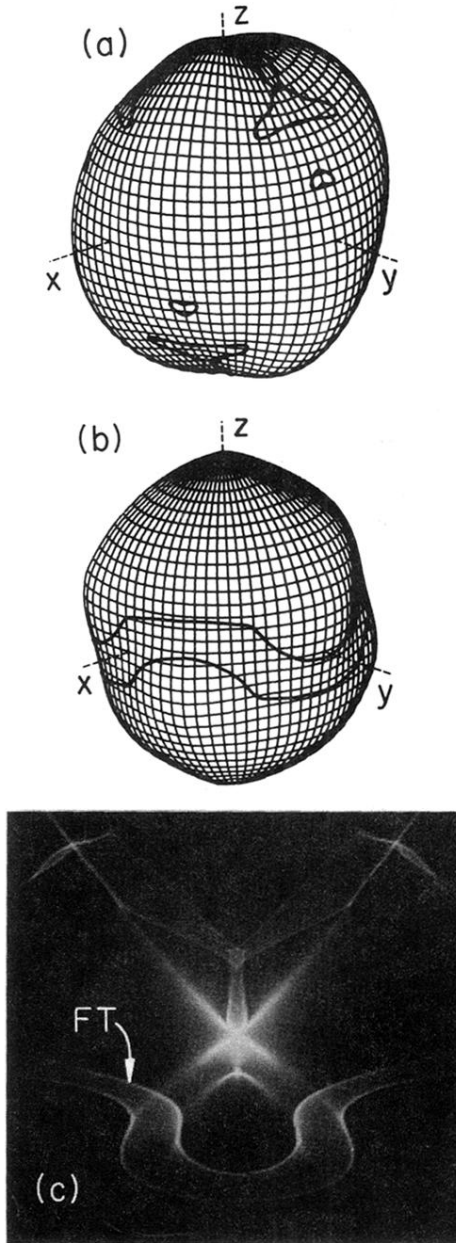


FIG. 2. Slowness surfaces obtained for LiNbO_3 , including the piezoelectric effect. (a) ST mode. (b) FT mode. (c) Predicted phonon-flux pattern extending $\pm 71^\circ$ horizontally and vertically.

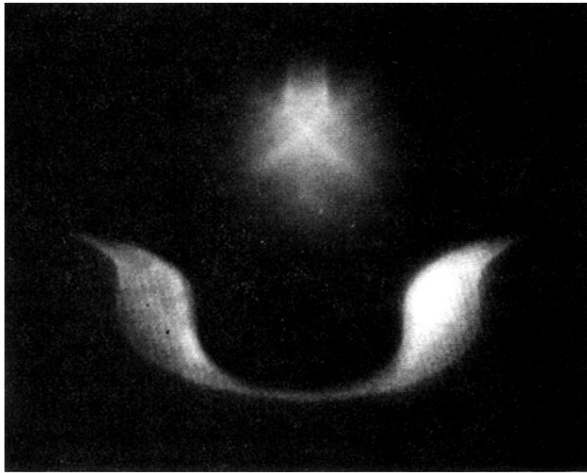


FIG. 3. Ballistic phonon image obtained with a broad time gate to include both ST and FT modes over a 50° range of propagation angles.